Earthquakes and Structures, *Vol. 16, No. 5 (2019) 575-588*
DOI: https://doi.org/10.12989/eas.2019.16.5.575

Component deformation-based seismic design method for RC structure and engineering application

Xiaolei Han*, Difang Huang[a], Jing Ji and Jinyue Lin

School of Civil and Transportation Engineering, South China University of Technology, Tianhe, Guangzhou, 510641, China

(Received November 15, 2018, Revised March 12, 2019, Accepted March 28, 2019)

Abstract. Seismic design method based on bearing capacity has been widely adopted in building codes around the world, however, damage and collapse state of structure under strong earthquake can not be reflected accurately. This paper aims to present a deformation-based seismic design method based on the research of RC component deformation index limit, which combines with the feature of Chinese building codes. In the proposed method, building performance is divided into five levels and components are classified into three types according to their importance. Five specific design approaches, namely, "Elastic Design", "Unyielding Design", "Limit Design", "Minimum Section Design" and "Deformation Assessment", are defined and used in different scenarios to prove whether the seismic performance objectives are attained. For the components which exhibit ductile failure, deformation of components under strong earthquake are obtained quantitatively in order to identify the damage state of the components. For the components which present brittle shear failure, their performance is guaranteed by bearing capacity. As a case study, seismic design of an extremely irregular twin-tower high rise building was carried out according to the proposed method. The results evidenced that the damage and anti-collapse ability of structure were estimated and controlled by both deformation and bearing capacity.

Keywords: component deformation-based; component deformation limit; design method; performance assessment; high-rise reinforced concrete structure; irregular building

1. Introduction

Although the concept of performance-based seismic design (PBSD) dates back to the 1980s (Sozen 1981), it is relatively new in practical engineering of tall and special buildings. Since the 1990s, performance-based earthquake engineering had evolved and been promoted by a series of recommendations, such as SEAOC vision 2000 report (1995), ATC 40 report (1996), FEMA series report 273 (1997), 274 (1997), 356 (2000), 343 (1999) and P-58 (2012), ASCE 41 standard 31 (2003), 41 (2006) and update of Elwood *et al.* (2007), CTBUH (2008), LATBSDC (2008), SEAOC (2007) and TBI (2010). With the development of society, people have a higher pursuit of architectural style and building function, which leads to more complex structural configuration and system beyond building code specification. Furthermore, to achieve a better decision making, seismic safety is no longer the only evaluation criterion of structural performance, stakeholders require more information about the casualties, probable repair cost, and time of occupancy interruption of their buildings under different levels of seismic hazard. In this context, PBSD gradually shows its superiority over code-based design approaches because traditional regulations are not applicable to special structures due to their unique behavior. Comparing to PBSD, traditional prescriptive design methods have several limitations: (1) terms are generally capable for regulating the design of low or medium rise buildings with common structural layout, and limitations of building height are specified; (2) rigid rules, such as structural indexes like period ratio and torsional displacement ratio, are imposed on structural design and analysis to ensure the safety of buildings, which may cause unreasonable results due to the conservatism; (3) inelastic behavior of structures under strong earthquake are taken into account in elastic analysis by prescribing seismic reduction factors, however, for tall buildings with unique structural behavior, these factors are impractical to be defined theoretically; (4) seismic performance of building under rare earthquake is guaranteed by force-based design method under frequent earthquake and specific seismic detailing, which is unable to reflect the damage state of structure quantitatively. Unlike the aforementioned drawbacks of traditional code-based design, PBSD provides a new way to subdivide the structural performance under various criteria so that more precise performance evaluation can be obtained (Moehle *et al.* 2011).

Various researches had been conducted to investigate and develop the theory of PBSD over the past decade. Methods had been proposed to evaluate structural performance from different perspectives. In the study by Mun and Yang (2016), a new flexural design approach of RC shear walls based on the displacement ductility ratio was presented, which established the relationship between simplified moment-curvature curve and displacement

*Corresponding author, Professor
E-mail: xlhan@scut.edu.cn
[a]Ph.D. Student
E-mail: rickyhuang8@outlook.com

ISSN: 2092-7614 (Print), 2092-7622 (Online)

ductility ratio so that performance of shear walls can be evaluated by displacement ductility ratio. Tian *et al.* (2016) conducted a comparative study on seismic resilience of two prototype tall buildings designed according to US code and Chinese code respectively, using the new generation seismic performance-based assessment method proposed by FEMA P-58. Lee and Jeong (2018) focused on the application of PBEE in lower seismicity regions in South Korea by introducing the seismic hazard of lower seismicity regions and presenting seismic evaluation of representative structures under this hazard. In the paper by Elif *et al.* (2015), seismic performance of Turkish residential buildings was assessed by a probabilistic method according to seismic damage and loss, expected number of casualties was utilized as the index to describe the structural performance. Based on the cost-effectiveness criterion and seismic hazard analysis, Tang *et al.* (2012) put forward a modified structural life-cycle cost model which considers both structural initial cost and the failure lost expectation on five performance levels. From these researches, various criteria had been adopted in evaluation of structural seismic performance, however, deformation-based seismic design method is the most common method in practical engineering because it is well intuitive and operable. Three levels of deformation, namely, structure level (e.g., interstory drift), component level (e.g., chord rotation or drift angle), material level (e.g., strain), are widely used as performance indication. Interstory drift is an important index of structure performance in current building codes. However, seismic damage investigations of previous earthquakes (Sharma *et al.* 2016, Lu *et al.* 2012) shown that columns with different axial load ratio exhibited different damage states, even failure patterns, in the same story, which indicates interstory drift is too general to describe damage states of building in some cases. Material strain reflects the local damage of structural components, but to obtain accurate strain requires refined meshing and material constitutive models, which increases computational cost dramatically in practical engineering. Comparing to interstory drift and strain, assessment based on component deformation achieves a balance between accuracy and efficiency. A large number of tests and analyses had been carried out to investigate the RC component performance, which provides a reliable foundation for establishing the relation among capacity, deformation and damage. In addition, current structural design method is forced-based section design at component level, therefore it is more transparent and operable for engineers to adopt component deformation as structural performance index.

Few building codes around the world have specific provision for PBSD of special structures. In a sense, the "three-level, two-stage" design system proposed in Chinses *Code for seismic design of buildings (GB5011-2010)* (2010) contained the idea of PBSD. However, the performance objectives specified are not precise enough, which only guarantee "operational under frequent earthquake, repairable under moderate earthquake, collapse safety under rare earthquake". To provide a guideline for evaluation and rehabilitation of existing buildings, FEMA 356 (2000) and ASCE 41 standard (2006) were proposed and deformation limits for deformation-controlled components were specified under three performance levels, i.e. IO, LS and CP. Nevertheless, these evaluation criteria are not suitable for the buildings in China because there exists huge difference in two design systems including seismic fortification intensity, material strength, seismic details, etc. On the other hand, a series of researches (Siahos and Dritsos 2010, Acun and Sucuoglu 2010, Ricci *et al.* 2012) indicated that the deformation limits in ASCE 41 are over conservative, which may cause excessive cost of strengthening even misleading evaluation results.

In this paper, a new method of Component Deformation-Based Seismic Design (CDBSD) is proposed, which makes it possible to evaluate the structural performance more realistically in nonlinear range and provide a quantitative assessment of structural performance from perspectives of strength and deformation. As a case study, the seismic performance of an irregular high rise building beyond the code specification was checked for rare earthquake by CDBSD, and brief analysis results and observation were summarized.

2. Component deformation-based seismic design method

2.1 Component deformation-based seismic design procedure

The key of CDBSD comprises of three parts: reasonable ground motion selection methodology, reliable nonlinear analysis and component deformation index limit, which ensures that performance of structure during an earthquake can be simulated and evaluated objectively. With the understanding of these essential parts, a general design procedure of CDBSD is established and divided into a series of tasks, as illustrated in Fig. 1.

1. Determine the building performance objectives. The structural engineers should discuss these performance criteria with the stakeholders and confirm the anticipated performance objectives after comprehensive consideration of the building importance, seismic hazard, seismic expected loss and repair cost estimation. These objectives will form an acceptable basis for design.

2. Preliminary Design is carried out by elastic response spectrum analysis in accordance with the building codes.

3. Select the appropriate earthquake records from ground motion database as the seismic input for nonlinear time-history analysis according to the structural dynamic properties.

4. Extract the internal force and deformation of components from time-history analysis results. Classify the failure modes and evaluate the damage state using bearing capacity and deformation. All the components should meet the requirements of their anticipated performance levels, otherwise adjustment of structural design is needed and return to step 2.

2.2 Building performance objectives and building performance levels

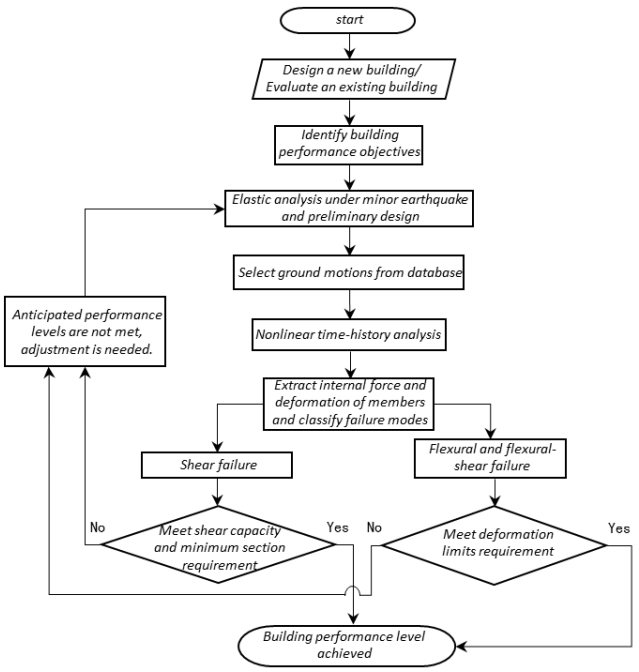

Fig. 1 Flowchart of component-deformation-based seismic design procedure

Table 1 Building performance matrix

Seismic Hazard Level	Building Performance Objectives			
	A	B	C	D
Frequent Earthquake	1	1	1	1
Moderate Earthquake	1	2	3	4
Rare Earthquake	2	3	4	5

A building performance matrix is specified in *Technical specification for concrete structures of tall building (JGJ3-2010)* (2010), as is shown in Table 1. In this matrix, building performance objectives have four levels, i.e. A, B, C, D respectively. And five Building Performance Levels (BPL), whose descriptions are given in Table 2, are defined as the anticipated seismic performance the structure should achieved at certain seismic hazard levels. As can be seen in Table 1, each building performance objective contains 3 BPLs corresponding to 3 seismic hazard levels, respectively. In CDBSD, different building performance levels require different design methods for components, which will be discussed below.

2.3 Deformation limits of components

As is implied by many seismic events and experimental results, damage of components and structures are tightly related to their deformations. Therefore, the component deformation is chosen as the index to determine the damage state in CDBSD. In order to establish the relationship among damage, bearing capacity and deformation of RC components, a series of researches (Ji *et al.* 2010, Qi *et al.* 2013, Parrotta *et al.* 2014) have been conducted to investigate the deformation capacity of RC beams, columns and shear walls. However, most research findings only remain theoretical rather than guiding practical engineering

Table 2 Qualitative description of building performance levels

Building Performance Level (BPL)	Description
1	All structural components remain in good condition. Buildings are operational without repairs.
2	Most structural components remain intact. Small cracks are observed in dissipative components. Buildings are operational under minor repairs.
3	Small cracks are observed in vertical components. Moderate damage occurs in part of dissipative components. Buildings are operational under ordinary repairs.
4	Most vertical components have minor cracks, some of them in obvious damage. Part of dissipative components experience serious damage. Buildings are not functional before strengthening and retrofit.
5	Most vertical components are in moderate damage, some of them are in serious damage. Dissipative components are in serious damage. Elimination of risk and rehabilitation are required for the building.

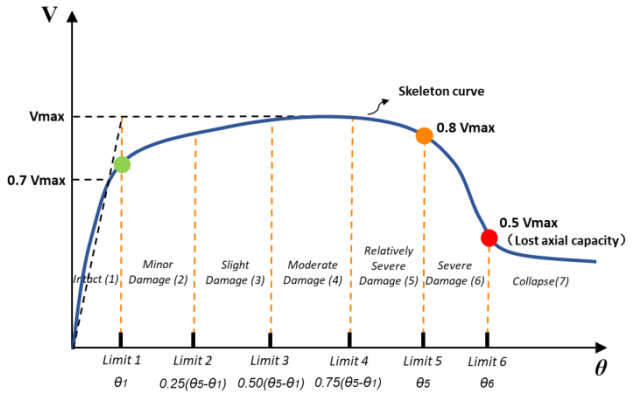

Fig. 2 Component performance levels and deformation limits

design. This situation is due to the following reasons: (1) most of the researchers only focus on the performance of certain types of components and their research findings separate with each other, the unified evaluation index system have not formed yet, (2) many differences exist in the material properties and code specific detailing of different countries, which leads to the difference of experimental results, (3) deformation limits proposed by existing specification are found very conservative compared to limits obtained from both experimental and analytical behavior (Elwood and Moehle 2006, Panagiotou *et al.* 2013).

Given the shortcoming noted above, Cui (2017) proposed a component performance evaluation method for RC beams, columns and shear walls based on skeleton curves, which is adopted for the seismic evaluation hereinafter. In this method, drift angle is chosen as the deformation index. 6 deformation limits are established, which divides the component performance into 7 states: “Intact”, “Minor Damage”, “Slight Damage”, “Moderate Damage”, “Relatively Severe Damage”, “Severe Damage” and “Collapse”, as illustrated in Fig. 2. Three key limits, namely, Limit 1, Limit 5 and Limit 6, are the basis of

Table 3 Design approaches of component

Building Performance Level (BPL)		Component Classification		
		Key Components	Vertical Component and Critical Frame Girder	Dissipative Component
1	Flexural & Axial	Elastic Design	Elastic Design	Elastic Design
	Shear	Elastic Design	Elastic Design	Elastic Design
2	Flexural & Axial	Elastic Design	Elastic Design	Unyielding Design
	Shear	Elastic Design	Elastic Design	Unyielding Design
3	Flexural &Axial	Unyielding Design /Deformation Assessment （B2, C2, SW2）	Unyielding Design /Deformation Assessment （B2, C2, SW2）	Limit Design /Deformation Assessment（B5）
	Shear	Elastic Design	Unyielding Design	Limit Design
4	Flexural &Axial	Deformation Assessment （B3, C3, SW3）	Deformation Assessment （B4, C4, SW4）	Deformation Assessment（B6）
	Shear	Unyielding Design	Limit Design	Minimum section design
5	Flexural &Axial	Deformation Assessment （B3, C3, SW3）	Deformation Assessment （B5, C5、SW5）	Deformation Assessment（B6）
	Shear	Limit Design	Minimum section design	Minimum section design

NOTES: B, C, SW represent the deformation limits of beam, column and shear wall respectively.

component performance partition. Limit 1 is the deformation at nominal yielding, which is calculated by the method proposed by Sezen and Moehle (2004). Components with deformation less than this limit remain elastic. Limit 5 is defined as the deformation at which the applied shear dropped to 80% of the maximum applied shear. When deformation reaches this limit, degeneration of lateral bearing capacity occurs but the component still able to withstand vertical loads stably. Limit 6 is defined as the deformation corresponding to the lost of component axial capacity. If axial capacity lost does not occur in the test or no axial loading is applied, Limit 6 can be defined as the deformation corresponding to 50% degradation of lateral bearing capacity. Once these three key limits are obtained, the overall deformation performance of component is established. Base on a database of 103 rectangular RC beams, 469 rectangular RC columns and 236 rectangular RC shear walls collected from published literatures, Cui *et al.* (2018a, 2018b) proposed new failure mode classification criteria of RC components. For each failure mode, i.e., flexural, flexural-shear, shear, three key limits were established through the regression analysis of sample data and verified by systematic component experiments. Limit 2, Limit 3 and Limit 4 are determined by quartering the deformation between Limit 1 and Limt 5, as shown in Fig. 2. Completed deformation limits tables for components in different failure modes are given in appendix. This deformation limit system provides an implementation for structure deformation evaluation under strong earthquake.

2.4 Design approaches of component under different Building Performance Levels

Seismic performance of structure can be enhanced by improving component bearing capacity or ductility. Components can be classified into three types according to their importance, namely, “Key Components”, “Vertical Components and Critical Frame Girder”, “Dissipative Component”. Different requirements of bearing capacity and ductility are assigned to different components. As shown in Table 3, performance of components under different Building Performance Levels (BPL) are ensured both in the case of flexural and shear by assigning corresponding design methods. On the basis of code-prescribed strength design method and RC component deformation limits mentioned above, five specific design methods are proposed here, which are “Elastic Design”, “Unyielding Design”, “Limit Design”, “Minimum Section Design” and “Deformation Assessment”, as shown in Table 3. At BPL 1 and BPL 2, as the structures almost remain in elastic range, strength design method based on elastic analysis is suitable, therefore Elastic Design and Unyielding Design are adopted. According to the macro and qualitative damage description in Table 2, structures gradually enter into elastic-plastic state from BPL 3, which means nonlinear analysis method is needed. At BPL 3, flexural performance can be checked by either bearing capacity or deformation, while at BPL 4 and BPL 5 flexural performance can only be checked by deformation since the component is already yielded. Component deformation should not exceed the corresponding deformation limits specified in Table 3. Generally, brittle shear failure is unacceptable in practical engineering, hence shear performance is assessed by bearing capacity. Five design methods are discussed hereinafter.

2.4.1 Elastic design

Elastic design applies to structures subject to frequent earthquake. Structural members should be designed considering most unfavorable combination of internal force determined by the following equation

$$\gamma_G S_{GE} + \gamma_{Eh} S_{Ehk} + \gamma_{Ev} S_{Evk} + \psi_w \gamma_w S_{wk} \le R_d / \gamma_{RE} \quad (1)$$

Where γ_G, γ_{Eh}, γ_{Ev}, γ_w are partial factors for gravity load, horizontal and vertical seismic action, wind load respectively. S_{GE}, S_{wk}, S_{Ehk}, S_{Evk} are effects resulting from representative value of gravity load, characteristic value of wind load, horizontal and vertical seismic action

respectively. ψ_w is the factor for combination value of wind load. R_d is the design value of load-bearing capacity of structural component.

When equivalent elastic design of structure is conducted under moderate or rare earthquake, internal force amplification factor of seismic effect and the effect of wind load should be neglected. The equation is

$$\gamma_G S_{GE} + \gamma_{Eh} S^*_{Ehk} + \gamma_{Ev} S^*_{Evk} \le R_d / \gamma_{RE} \quad (2)$$

Where S^*_{Ehk}, S^*_{Evk} are the effect for characteristic value of horizontal and vertical seismic action respectively without considering amplification factor of internal force.

2.4.2 Unyielding design

Unyielding design aims to calculate the component bearing capacity in a critical state before yielding. In unyielding design under moderate earthquake or rare earthquake, characteristic value of material strength is adopted, the bearing capacity of structural components should comply with Eq. (3).

$$S_{GE} + S^*_{Ehk} + 0.4 S^*_{Evk} \le R_k \quad (3)$$

Where R_k is the characteristic value of load-bearing capacity of structural component.

2.4.3 Limit design

In limit design, bearing capacity of structural members should be calculated using mean value of material strength, which should comply with Eq. (4).

$$S_{GE} + S^*_{Ehk} + 0.4 S^*_{Evk} \le R_u \quad (4)$$

Where R_u is the ultimate value of bearing capacity of structural members using mean value of material strength, which can be obtained from component experiments.

2.4.4 Minimum section design

Minimum section design is the minimum requirement to prevent the occurrence of brittle shear failure. The section of RC components should comply with Eq. (5).

$$V_{GE} + V^*_{Ek} \le 0.15 f_{ck} b h_0 \quad (5)$$

Where V_{GE} and V^*_{Ek} are the shear force induced by representative value of gravity load and characteristic value of seismic action respectively, which can be obtained from nonlinear analysis or equivalent elastic analysis. And f_{ck} is the characteristic value of concrete compression strength.

2.4.5 Deformation assessment

Experimental results evidence that damage of structural components can be reflected by deformation, therefore the damage state of components can be evaluated and controlled by deformation limits of components. The equation can be expressed as follow

$$\delta \le [\delta] \quad (6)$$

Where δ is the deformation demand in certain earthquake hazard level and $[\delta]$ is the deformation limits of corresponding component performance levels.

Fig. 3 Architectural rendering of the building

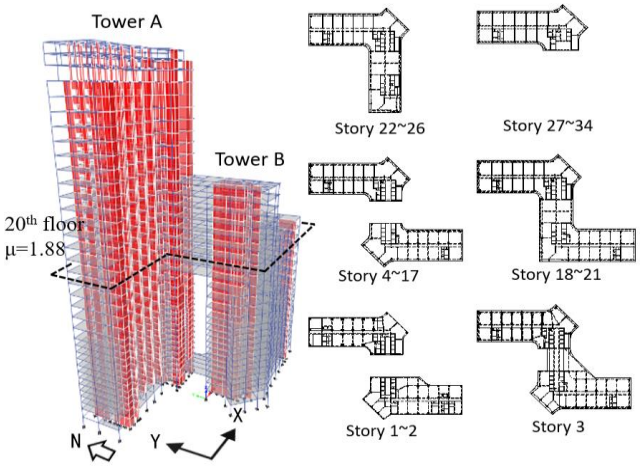

Fig. 4 Schematic 3D view of the structural model

3. Engineering application

To prove the validity and feasibility of CDBSD, structural design procedure of an extremely irregular high-rise building completed in accordance with this method was presented hereinafter; brief analysis results and observations were summarized.

3.1 Structural system

The integrated office building was planned to be constructed in Shantou, Guangdong province and the architectural rendering is given in Fig. 3. Seismic fortification intensity of this region is degree 8 with design peak ground acceleration of 0.2 g and the site classification is type III. Due to the architectural design requirements, this building has extremely irregular structural layout. As illustrated in Fig. 4, this structure consists of two individual towers (Tower A and Tower B) connected at story 3 and story 18~26. Tower A, a frame-supported shear wall structure with 34 stories, has a total height of 149.5 m. The transfer story is located at third floor where 8 shear walls are supported by reinforced concrete girders, as illustrated in Fig. 5(a). Tower B is a frame shear wall structure with 25 stories and it has a height of 104.5 m. There exist two significant elevation setbacks in this structure while the first setback takes about 30% of the plan at 22nd floor (79.7 m)

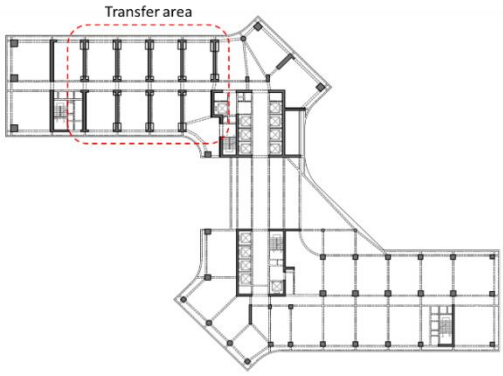

(a) Structural layout of transfer story

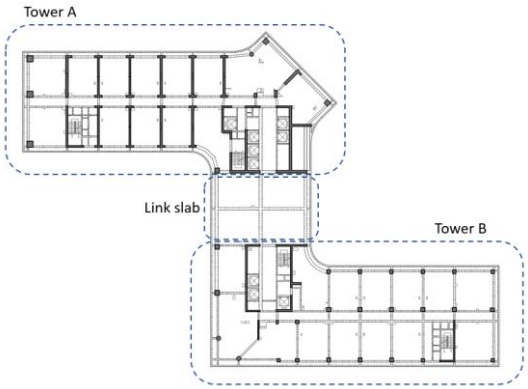

(b) Structural layout of connected story

Fig. 5 Typical floor plan

and the second one takes about 42% at 26th floor (104.5 m), as shown in Fig. 4.

3.2 Design challenges

Due to the architectural requirement, this building was designed as a twin-tower high rise building. There are three design challenges which are, briefly, a) complex connection caused by the significant difference in dynamic behavior of two towers, b) discontinuity of vertical members induced by transfer story which leads to sharp change in vertical stiffness and load paths, c) severe torsion effect caused by extreme irregular plan, the maximum torsional displacement ratio reaches 1.88, which far exceeds code limits of 1.2. It is obvious that the current seismic design codes are not fully suitable for this building, therefore, CDBSD is adopted here to evaluate the structural performance.

3.3 Determination of building performance objectives

Considering the design conditions and economic benefit, Level C in Table 1 was selected as the anticipated building performance objective, which means this building should achieve BPL 1 under frequent earthquake, BPL 3 under moderate earthquake and BPL 4 under rare earthquake. Performance levels and design methods of different components were refined according to the importance and building performance objective respectively, as shown in Table 4.

Table 4 Seismic performance level of structure and component

Structural Performance	Seismic Hazard Level		Frequent Earthquake	Moderate Earthquake	Rare Earthquake
	Building Performance Level (BPL)		1	3	4
	Interstory Drift		1/800	——	1/100
Key Components	Shear Walls in Critical Region	shear	Elastic	Elastic	Unyielding
		flexural	Elastic	Unyielding	Slight damage*
	Columns in Critical Region	shear	Elastic	Elastic	Unyielding
		flexural	Elastic	Unyielding	Slight damage*
	Transfer Girders and Frame-supported columns	shear	Elastic	Elastic	Unyielding
		flexural	Elastic	Unyielding	Slight damage*
	Components in Connected Region	shear	Elastic	Elastic	Unyielding
		flexural	Elastic	Unyielding	Slight damage*
Vertical Components and Critical Frame Girder	General Shear Walls	shear	Elastic	Unyielding	Unyielding
		flexural	Elastic	Unyielding	Moderate damage*
	General Columns	shear	Elastic	Unyielding	Unyielding
		flexural	Elastic	Unyielding	Moderate damage*
Dissipative Components	Frame Beams	shear	Elastic	Unyielding	Minimum section
		flexural	Elastic	Limit	Moderate damage*
	Coupling Beams	shear	Elastic	Unyielding	Minimum section
		flexural	Elastic	Limit	Severe damage*
Slabs of the Setback Stories (Story 21 and 26) and the Connected Stories (Story 3 and 18~26)		shear	Elastic	Unyielding	—
		tension	Elastic	Unyielding	—

NOTES: Items with * means deformation controlled.

Table 5 Selected ground motions

GM No.	Earthquake name	Event	Date	Magnitude
GM1	NGA_no_143_ TAB-TR_RS	Tabas, Iran	1978/ 09/16	7.35
GM2	NGA_no_178_ H-E03230_RS	Imperial Valley-06	1979/ 10/15	6.53
GM3	NGA_no_1170_ MCD090_RS	Kocaeli, Turkey	1999/ 08/17	7.51
GM4	NGA_no_1605_ DZC270_RS	Duzce, Turkey	1999/ 11/12	7.14
GM5	NGA_no_1786_ 22T04090_RS	Hector Mine	1999/ 10/16	7.13
GM6	Artificial seismic motion 1	-	-	-
GM7	Artificial seismic motion 2	-	-	-

3.4 Site specific assessment of seismic hazard

According to the *Seismic ground motion parameter zonation map (GB18306-2015)* (2015), the construction site is located in the area with the condition of degree 8 of seismic fortification intensity (PGA=0.2 g). Having shear wave velocity of 250 m/s, the soil in this site belongs to type III in Chinese code GB50011-2010, which is

Table 6 Peak ground acceleration (PGA) and seismic influence coefficient under different earthquake levels

Earthquake level	Probability of exceedance	PGA (g)	Seismic influence coefficient α_{max}
Frequent earthquake	64% in 50 years	0.07	0.16
Moderate earthquake	10% in 50 years	0.2	0.45
Rare earthquake	2~3% in 50 years	0.4	0.90

Table 7 Periods of structure

Vibration mode	Period (s)	Translational Factor (X+Y)	Torsional Factor
T_1	4.41	0.94(0.90+0.04)	0.06
T_2	3.34	0.77(0.13+0.64)	0.23
T_3	2.72	0.51(0.10+0.41)	0.49
T_4	1.60	0.92(0.91+0.01)	0.08
T_5	1.24	0.28(0.18+0.10)	0.72
T_6	0.91	0.95(0.01+0.94)	0.05

approximately corresponding to Site Class D in ASCE 7 (2016). Seven strong ground motions, entitled GM1~GM7, were selected for time history analysis and their information is listed in Table 5. It should be noted that GM1~GM5 are real ground motion records in different events while GM6 and GM7 are artificial seismic motions generated according to design response spectrum (GB 50011-2010 2010). Time histories of the selected ground motions are given in Fig. 6 and all records have been scaled according the peak acceleration of 0.07 g, which is the specified PGA for frequent earthquake in seismic region with intensity 8 (GB 50011-2010 2010). The design response spectrum of frequent earthquake level for 5% damping as well as elastic response spectra of each selected ground motions are shown in Fig. 7. Peak ground acceleration (PGA) and seismic influence coefficients for time history analysis are listed in Table 6.

3.5 Linear elastic seismic analysis

Elastic analyses under frequent earthquake and moderate earthquake were carried out by ETABS (2016). Preliminary design of section size and reinforcement was conducted according to analysis results. Bearing capacity demands of components are all fulfilled when the structure subject to frequent earthquake. In regard to dynamic behavior, 30 vibration modes were considered during the calculation. Modal participation factor in direction X is 97.36% while the factor in direction Y is 95.62%. The periods and modal direction factors which identify the predominant direction of the first 6 vibration modes are given in Table 7. As illustrated in Fig. 8, the first and the second modes mainly consist of translational components in two horizontal directions while the third mode is a torsional mode.

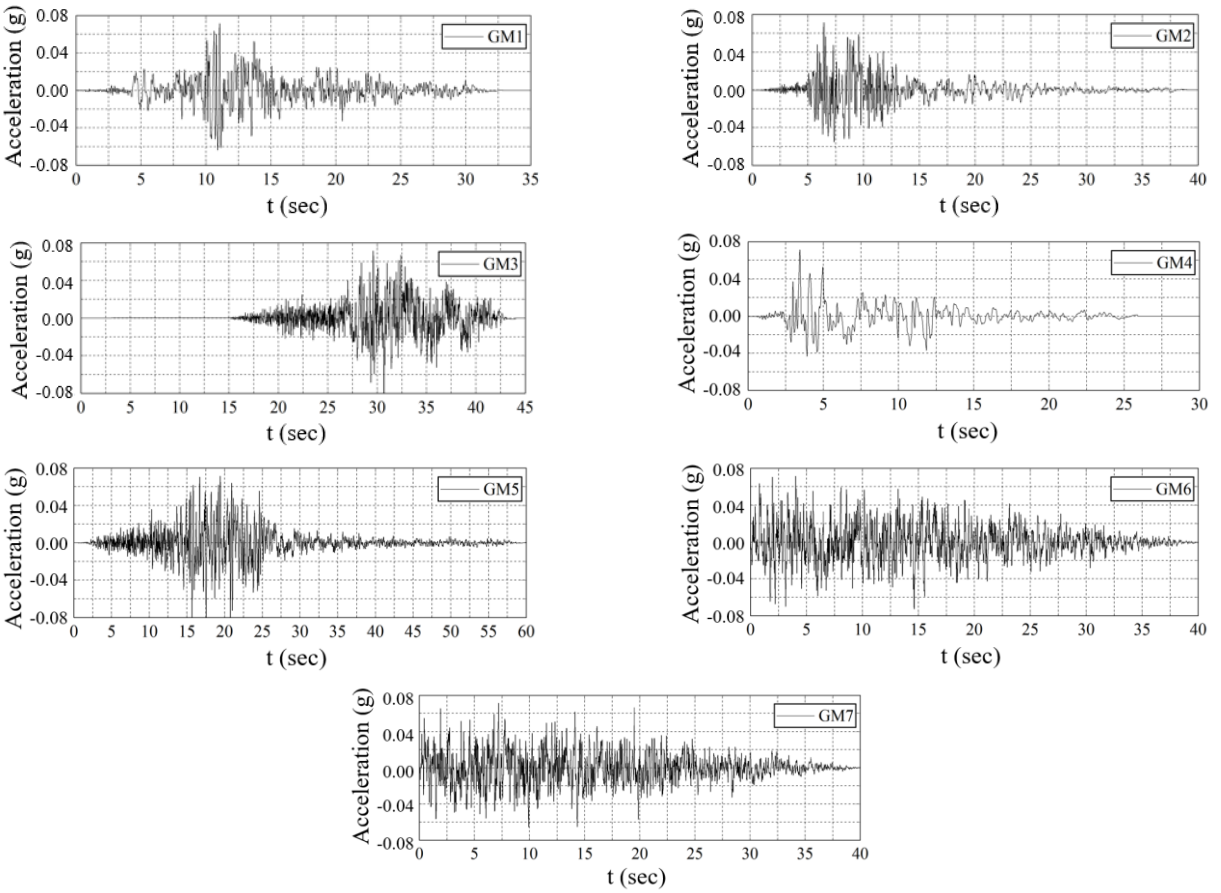

Fig. 6 Time-histories of selected ground motions

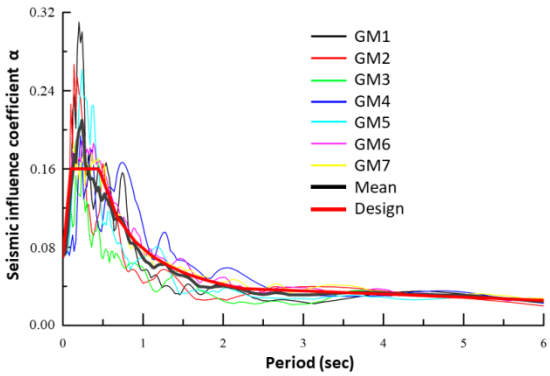

Fig. 7 Design response spectrum for 5% damping and elastic spectra for selected ground motions

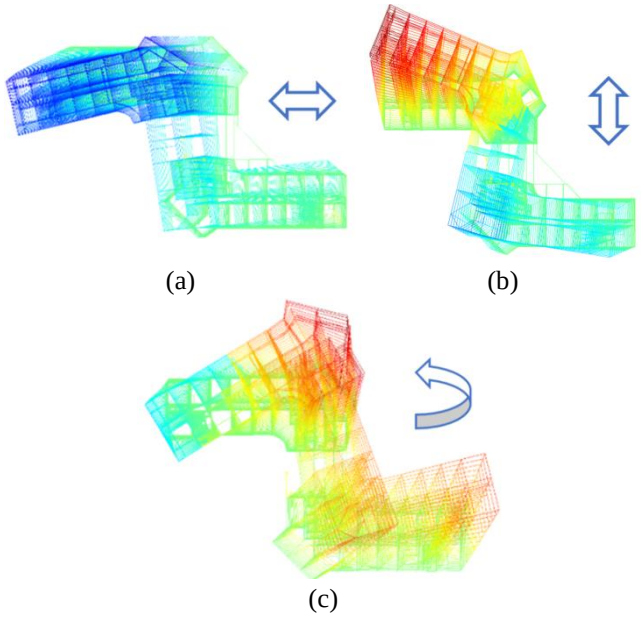

Fig. 8 First three vibration modes of the building: (a)first mode; (b)second mode; (c) third mode

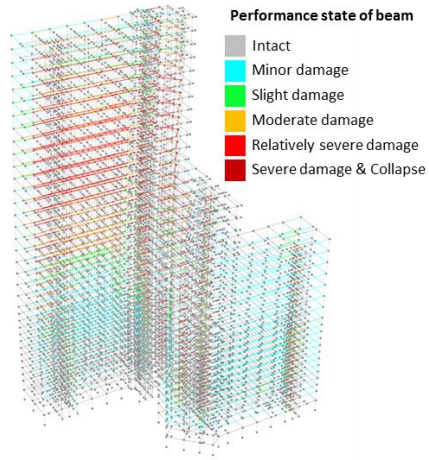

(a)

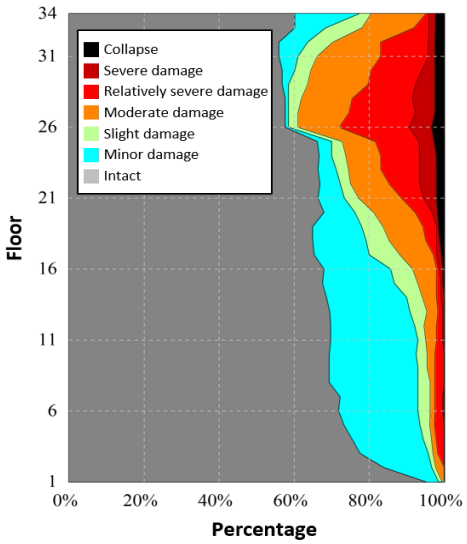

(b)

Fig. 9 Performance states of beams under GM4-X: (a) Distribution of different performance states (b) Proportion of different performance state of different floors

3.6 Nonlinear time-history analyses and performance evaluation

Seismic performance was checked for rare earthquake by PERFORM-3D (2011). Key points of nonlinear time-history analysis are summarized as below:

a) Columns and beams were modeled utilizing Frame Member Compound Component with inelastic fiber section while shear walls were modeled by Shear Wall Compound Component based on MVLEM theory (Wallace *et al.* 2006). Reinforcement of members were input according to the results of preliminary elastic design.

b) Elastic shell element was utilized for simulating the linked slabs in connected region. Rigid diaphragms were assigned to Tower A and Tower B separately in order to consider axial forces of beams and in-plane stresses of linked slabs more realistically.

c) Selected ground motions were input bi-directionally (*X* and *Y*) for the time-history analysis, while the peak ground acceleration ratio between primary direction and secondary direction was 1:0.85.

Component performance was checked from shear and flexural aspects respectively. It is observed from the nonlinear analysis results that the requirements of component shear capacity specified in Table 3 are satisfied. In order to get a general understanding of the damage of the structure, analysis result under rare earthquake GM4-X is used as an example to illustrated the distribution of component performance. Components in different performance levels are depicted and percentage of each performance level in each floor is summarized, as shown in Figs. 9-11. For dissipative components including frame beams and couple beams, most of them remain Intact. In lower floors like 1~18th floor, about 20% of the beams reach Minor Damage level while less than 10% are in worse condition. In 18~26th floor, which is the connected region, the damage increases remarkably due to the accommodation of deformation between two towers. And a steep increase is observed at 26th floor because of the second elevation setback. Although the proportion of damaged components

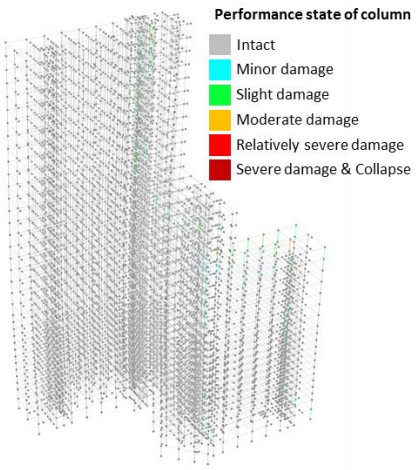

(a)

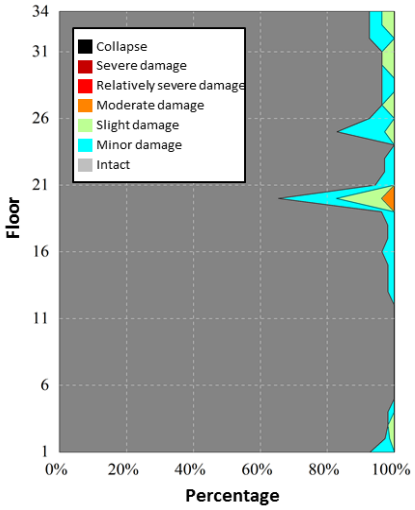

(b)

Fig. 10 Performance states of columns under GM4-X: (a) Distribution of different performance states (b) Proportion of different performance state of different floors

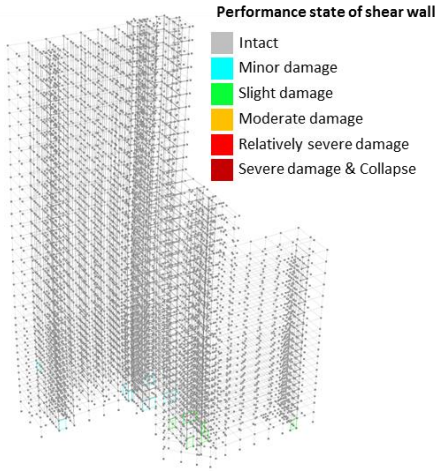

(a)

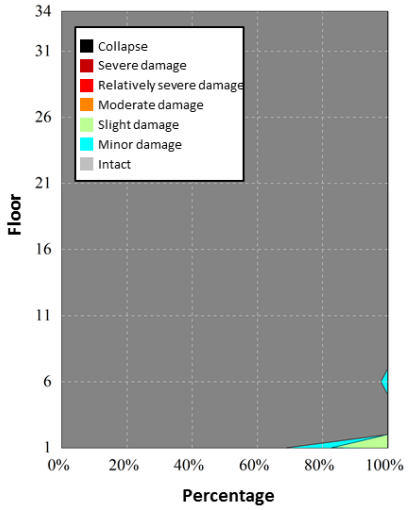

(b)

Fig. 11 Performance states of shear walls under GM4-X: (a) Distribution of different performance states (b) Proportion of different performance states in different floors

gradually decline in the region above 26th floor, this region suffers the most serious damage. It is worth noting that coupling beams adjacent to the connected region is the part damaged most seriously. Maximum drift angle exceeded limit B5, reaching the Severe Damage state. Some of them are even in Collapse state, as shown in Fig. 9(a). With regard to columns, as can be seen from Fig. 10(b), most of the columns are in Intact level while only a very few columns reach Moderate Damage state. And the damaged columns mainly distribute in 20th floor and 25th floor, where is the location of the first and second elevation setback respectively. As for shear walls, Fig. 11 indicates that all components remain Intact except for the first floor where 12% in Minor Damage level while 18% in Slight Damage level. In general, under the rare earthquake of seismic intensity degree 8, frame beams and couple beams suffered the most serious damage, and input seismic energy were dissipated by the deformation at the same time. Therefore, vertical components including columns and shear walls were still in good condition and no local collapse was observed, which conforms to the anticipated design idea.

3.7 Verification of key component performance

To get more insight into the structural performance, deformation time history of key components in critical regions were extracted for evaluation. For this structure, key components are mainly in three parts: a) the transfer columns and transfer girders in 3rd floor, b) frame beams supporting link slab in the connected region, and c) the columns in the floor with obvious torsional effect. It is observed that the torsional displacement ratio$\mu$of 20th floor reaches 1.88 under rare earthquake in *Y* direction considering accidentally eccentricity, which far exceeds the limit of 1.2 in Chinese building code (GB 50011-2010, 2010), as shown in Fig. 4. Therefore, a more accurate review of performance in component level is needed. Deformation time histories of most seriously damaged components in three critical regions are given in Figs. 13-20. As can be seen from Figs. 13-14, transfer columns and girders in 3rd floor are all in Intact state. In connected region, frame beam KL5 in 21st floor experience the maximum plastic rotation angle of and enter Minor Damage

Table 8 Shear capacity assessment of RC columns (kN)

Component No.	Seismic	GM1	GM2	GM3	GM4	GM5	GM6	GM7	Average	Unyielding Capacity
NKZ1	*X*	433.2	457.2	403.2	396	410.4	427.2	404.4	419	6122
	Y	360	408	334.8	279.6	306	327.6	345.6	337	6207
NKZ4	*X*	336	361.2	304.8	294	320.4	351.6	294	323	5967
	Y	320.4	312	296.4	351.6	328.8	361.2	380.4	336	6017
SKZ3	*X*	556.8	490.8	445.2	620.4	434.4	511.2	505.2	509	1927
	Y	843.6	861.6	828	874.8	844.8	865.2	866.4	855	1879
SKZ4	*X*	298.8	273.6	310.8	324	291.6	315.6	310.8	304	1123
	Y	386.4	418.8	370.8	415.2	378	410.4	436.8	402	1120
SKZ5	*X*	322.8	298.8	308.4	339.6	290.4	325.2	338.4	318	1122
	Y	297.6	342	292.8	277.2	284.4	274.8	262.8	290	1117
NZHZ1	*X*	1824	1876.8	1411.2	1849.2	1857.6	1778.4	1903.2	1786	8474
	Y	2077.2	1910.4	1764	2109.6	2504.4	2530.8	2352	2178	10517
NKZL3	*X*	2597	2738	2641	2571	2581	2547	2594	2610	2808
	Y	2232	2286	2068	2309	2187	2165	2390	2234	2808
KL5	*X*	866	858	809	869	848	840	924	859	1008
	Y	787	754	689	775	743	712	833	756	1008

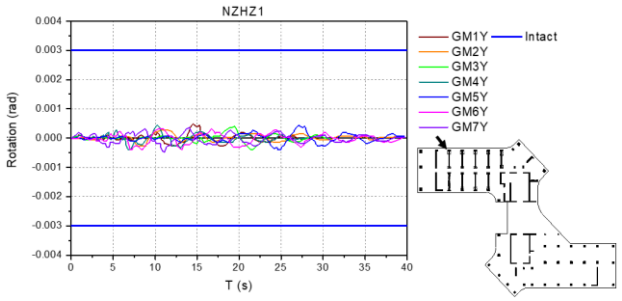

Fig. 13 Deformation time-history of transfer column NZHZ1

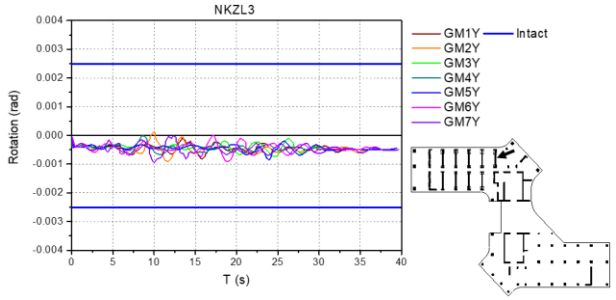

Fig. 14 Deformation time-history of transfer girder NKZL3

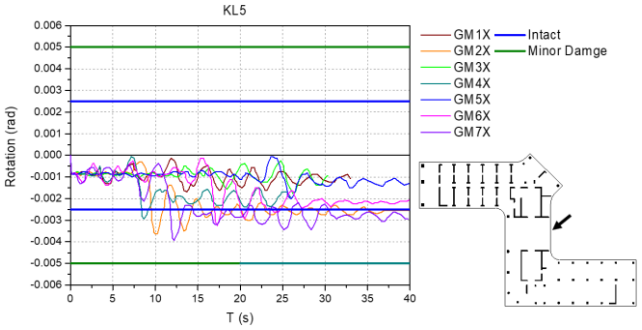

Fig. 15 Deformation time-history of connected beam KL5

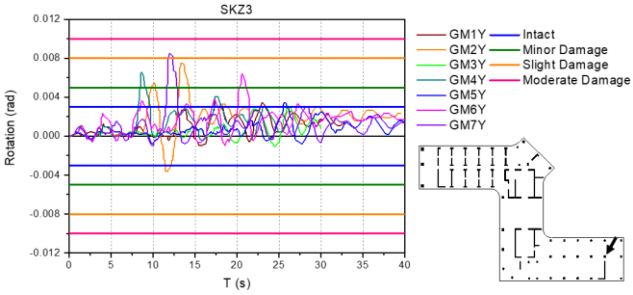

Fig. 16 Deformation time-history of column SKZ3

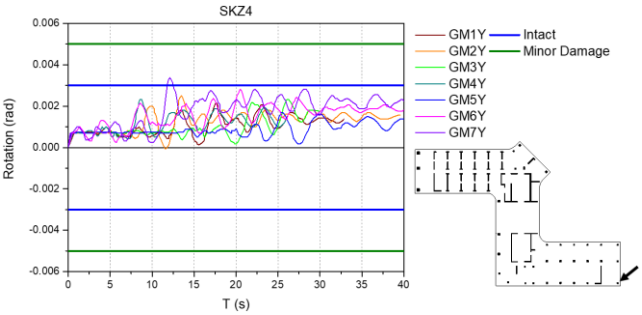

Fig. 17 Deformation time-history of column SKZ4

state, as depicted in Fig. 15. The corner columns NKZ1, NKZ4, SKZ3, SKZ4 and SKZ5 in story 20, as can be seen from Fig. 12, which are far away from the center of stiffness, should be one of the most critical parts of the structure due to the shear force and large deformation caused by significant torsional effect. However, time histories shown in Figs. 16-20 indicates that the most critical column is SKZ3, which reaches Moderate Damage state, and the rest are all in Minor Damage or Intact state. Table 8 indicates that the shear forces of these members under rare earthquake are all lower than the shear capacity calculated in Unyielding Design, which guaranteed shear failure will not occur. Based on the result of bearing capacity and deformation evaluation, it can be concluded that although this structure has a considerable torsional effect, the deformation and damage of the components actually remain in an acceptable range and the structural safety under rare earthquake is guaranteed. It also proves

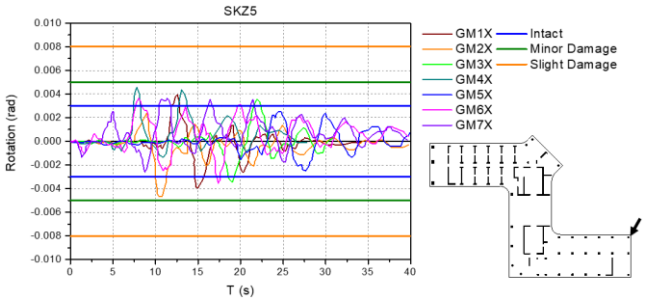

Fig. 18 Deformation time-history of beam SKZ5

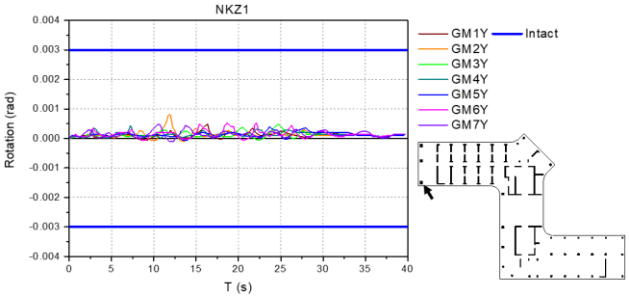

Fig. 19 Deformation time-history of coupling beam NKZ1

that the structural indexes specified in prescriptive codes are not suitable for structures with unique behavior because of their conservatism.

4. Conclusions

To provide a transparent platform for stakeholders and engineers to decide the expected seismic performance of structure under different earthquake hazard levels, a component deformation-based method was proposed based on the deformation limits of RC components. As a typical case study, the seismic evaluation of an irregular high-rise building was conducted to prove the validity and feasibility of CDBSD. The following conclusion may be drawn.

- Instead of ensuring prescribed ductility and bearing capacity through elastic design and seismic detailing, the seismic performance of building was analyzed and evaluated at component level in CDBSD, which may capture the real behavior reasonably. By adopting the deformation limits of RC components, the relationship between damage state and component deformation had been established. Performance levels were quantified with consideration of component types, failure modes and different design approaches. Through the analysis of component damage distribution, engineers may have more confidence in structural performance under various levels of earthquake excitation. Since this method is based on components rather than structures, it is applicable to not only tall and complex buildings but also ordinary buildings like multistory RC frames.
- Although the structure suffered a significant torsional effect, it was observed from the deformation of key components that the damage in critical regions remained in an acceptable range, which indicates that prescriptive design method is not suitable for seismic performance evaluation of these special structures. In some cases, meeting the requirement of conservative structural indexes may leads to a waste of materials even design error.
- Due to the diversity of the structural systems and layouts of modern buildings beyond code specification, it is difficult to represent their unique structural behavior by several typical examples. The expertise of engineers still plays an important role in the judgement of structural performance. A more in-depth study of the relationship between components performance state and structural performance state is needed.

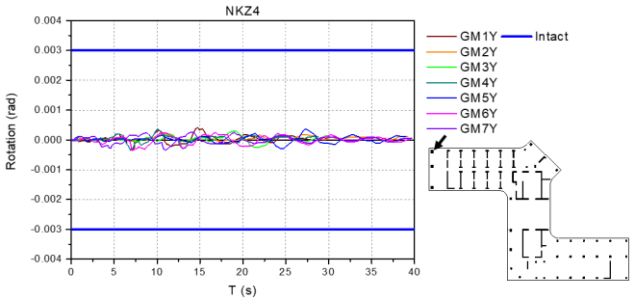

Fig. 20 Deformation time-history of column NKZ4

Acknowledgements

The research described in this paper is financially supported by Natural Science Foundation of Guangdong Province (2017A030313274/2017A030313306) and NSFC (National Natural Science Foundation of China) (51378221).

References

Acun, B. and Sucuoglu, H. (2010), "Performance of reinforced concrete columns designed for flexure under severe displacement cycles", *ACI Struct. J.*, **107**, 364-371.

ASCE/SEI 31 (2003), Seismic Evaluation of Existing Buildings, American Society of Civil Engineers, Reston, Virginia, USA.

ASCE/SEI 41 (2006), Seismic Rehabilitation of Existing Buildings, American Society of Civil Engineers, Reston, Virginia, USA.

ASCE/SEI 7 (2016), Minimum Design Loads for Buildings and Other Structures, American Society of Civil Engineers: Reston, Virginia, USA.

ATC-40 (1996), Seismic Evaluation and Retrofit of Concrete Buildings. Applied Technology Council, Redwood, California, USA.

CTBUH (2008), Recommendations for the Seismic Design of High-rise Buildings, Council on Tall Buildings and Urban Habitat, Illinois Institute of Technology, Chicago, USA.

Cui, J.D. (2017), "Research and experimental verification of deformation index limits of RC beams, columns and shear walls", Ph.D. Dissertation, South China University of Technology, Guangzhou, China.

Cui, J.D., Han, X.L., Gong, H.J. and Ji, J. (2018b), "Deformation limits of reinforces concrete columns and their experimental verification", *J. Tongji Univ. (Nat. Sci.)*, **46**(5), 593-603.

Cui, J.D., Han, X.L., Ji, J. and Gong, H.J. (2018a), "Experimental

study on deformation limits of RC beams", *J. Harbin Inst. Technol.*, **50**(6), 169-176.

Elif, M.U., Erberik, M.A. and Askan, A. (2015), "Performance assessment of Turkish residential buildings for seismic damage and loss estimation", *J. Perform. Constr. Facil.*, **29**(2), 04014063. https://doi.org/10.1061/(ASCE)CF.1943-5509.0000547.

Elwood, K.J. and Moehle, J.P. (2006) "Idealized backbone model for existing reinforced concrete columns and comparisons with FEMA 356 criteria", *Struct. Des. Tall Spec. Build.*, **15**, 553-569. https://doi.org/10.1002/tal.382.

Elwood, K.J., Matamoros, A., Wallace, J.W., Lehman, D., Heintz, L., Mitchell, A., Moore, M., Valley, M., Lowes, L.N., Comartin, C. and Moehle, J.P. (2007) "Update to ASCE/SEI 41 concrete provisions", *Earthq. Spectra*, **23**(3), 493. https://doi.org/10.1193/1.2757714.

ETABS (2016), Extended 3D Analysis of Building Systems Software, Computers and Structures, Inc., Berkeley, CA, USA.

FEMA 273 (1997), NEHRP Guidelines for Seismic Rehabilitation of Buildings, Federal Emergency Management Agency: Washington, D.C., USA.

FEMA 274 (1997), NEHRP Commentary on the guidelines for seismic rehabilitation of buildings, Federal Emergency Management Agency, Washington, D.C., USA.

FEMA 343 (1999), Case Studies: An Assessment of the NEHRP guidelines for the seismic rehabilitation of buildings, Federal Emergency Management Agency, Washington, D.C., USA.

FEMA 356 (2000), Prestandard and Commentary for the Seismic Rehabilitation of Buildings, Federal Emergency Management Agency, Washington, D.C., USA.

FEMA P-58-1 (2012), Seismic Performance Assessment of Buildings Volume 1- Methodology, Washington, D.C., USA.

GB 50011-2010 (2010), Code for Seismic Design of Buildings, Architecture & Building Press, Beijing, Ministry of Housing and Urban-Rural Development of the P.R. China, China.

GB18306-2015 (2015), General Administration of Quality Supervision, Inspection and Quarantine of P.R.C, Seismic Ground Motion Parameter Zonation Map, Architecture & Building Press, Beijing, China.

JGJ3-2010 (2010), Technical Specification for Concrete Structures of Tall Building, Architecture & Building Press, Beijing, Ministry of Housing and Urban-Rural Development of the P.R. China, China.

Ji, J., Xiao, Q. and Huang, C. (2010), "Research on deformation limits of performance-based RC shear walls controlled by flexure", *J. Build. Struct.*, **31**(9), 35-41.

LATBSDC (2008), An Alternative Procedure for Seismic Analysis and Design of Tall Buildings Located in the Los Angeles Region, Los Angeles Tall Buildings Structural Design Council: Los Angeles, CA, USA.

Lee, H.S. and Jeong, K.H. (2018), "Performance-based earthquake engineering in a lower-seismicity region: South Korea", *Earthq. Struct.*, **15**(1), 45-65. https://doi.org/10.12989/eas.2018.15.1.045.

Lu, X., Ye, L., Ma, Y. and Tang, D. (2012), "Lessons from the collapse of typical RC frames in Xuan-kou school during the Great Wen-chuan Earthquake", *Adv. Struct. Eng.*, **15**(1), 139-153. https://doi.org/10.1260/1369-4332.15.1.139.

Moehle, J., Bozorgnia, Y., Jayaram, N., Jones, P., Rahnama, M., Shome, N., Tuna, Z., Wallace, J., Yang, T. and Zareian. F. (2011), "Case studies of the seismic performance of tall buildings designed by alternative means", PEER Report 2011/05, Pacific Earthquake Engineering Research Center, Berkeley, CA, USA.

Mun, J. and Yang, K. (2016), "Displacement ductility ratio-based flexural design approach of reinforced concrete slender shear walls", *Mag. Concrete Res.*, **68**(8), 409-422. https://doi.org/10.1680/jmacr.15.00113.

Panagiotou, M., Visnjic, T., Antonellis, G., Galanis, P. and Moehle, J.P. (2013), "Effect of hoop reinforcement spacing on the cyclic response of large reinforced concrete special moment frame beams", PEER Report 2013/16, Pacific Earthquake Engineering Research (PEER) Center, College of Engineering, University of California, USA.

Parrotta, J.E., Peiretti, H.C., Gribniak, V. and Caldentey, A.P. (2014), "Investigating deformations of RC beams: experimental and analytical study", *Comput. Concrete*, **13**(6), 1-27. https://doi.org/10.12989/cac.2014.13.6.799.

PERFORM 3D (2011), Nonlinear Analysis and Performance Assessment for 3D Structures User Guide, Version 5, Computers and Structures, Inc., Berkeley, CA, USA.

Qi, Y.L., Han, X.L. and Ji, J. (2013), "Failure mode classification of reinforced concrete column using Fisher method", *J. Central South Univ.*, **20**, 2863-2869. https://doi.org/10.1007/s11771-013-1807-1.

Ricci, P., Verderame, G. and Manfredi, G. (2012), "ASCE/SEI 41 Provisions on deformation capacity of older-type reinforced concrete columns with plain bars", *J. Struct. Eng.*, **139**, 04013014. https://doi.org/10.1061/(ASCE)ST.1943-541X.0000701.

SEAONC (2007), Requirements and Guidelines for the Seismic Design and Review of New Tall Buildings using Non-prescriptive Seismic-Design Procedures, Structural Engineers Association of Northern California, San Francisco, CA, USA.

Sezen, H. and Moehle, J.P. (2004), "Shear strength model for lightly reinforced concrete columns", *J. Struct. Eng.*, **130**(11), 1692-1703. https://doi.org/10.1061/(ASCE)0733-9445(2004)130:11(1692).

Sharma, K., Deng, L. and Noguez, C.C. (2016), "Field investigation on the performance of building structures during the April 25, 2015 Gorkha earthquake in Nepal", *Eng. Struct.*, **121**, 61-74. https://doi.org/10.1016/j.engstruct.2016.04.043.

Siahos, G. and Dritsos, S. (2010), "Procedural assumption comparison for old buildings via pushover analysis including the ASCE 41 update", *Earthq. Spectra*, **26**, 187-208. https://doi.org/10.1193/1.3272266.

Sozen, M.A. (1981), "Review of earthquake response of RC buildings with a view of drift control", *State of the Art in Earthquake Engineering, Proceedings of the 7th World Conference on Earthquake Engineering*, Istanbul, Turkey January.

Tang, Y., Zheng, Q. and Lou, M. (2012), "Optimization of seismic performance objectives based on cost-effectiveness criterion", *J. Tongji Univ. (Nat. Sci.)*, **40**(11), 1613-1619.

TBI (2010), "Guidelines for performance-based seismic design of tall buildings", PEER Report 2010/05, The TBI Guidelines Working Group, Pacific Earthquake Engineering Research Center, University of California, Berkeley, California, USA.

Tian, Y., Lu, X., Lu, X., Li, M. and Guan, H. (2016), "Quantifying the seismic resilience of two tall buildings designed using Chinese and US Codes", *Earthq. Struct.*, **11**(6), 1-19. https://doi.org/10.12989/eas.2016.11.6.925.

Vision 2000 (1995), Performance Based Seismic Engineering of Buildings, Structural Engineers Association of California, Oakland, USA.

Wallace, J.W., Massone, L.M. and Orakcal, K. (2006), "Analytical modeling of reinforced concrete walls for predicting flexural and couple-shear-flexural responses", PEER Report 2006/07, Pacific Earthquake Engineering Research (PEER) Center, College of Engineering, University of California, California, USA.

CC

Notations

λ	shear span ratio of the component, which can be calculated by $\lambda=L_a/h_0\approx M/Vh_0$
m	flexural shear ratio of the component, which can be calculated by $m=M_n/V_nL_a$
L_a	effective length of the cantilever.
M	moment at cantilever end.
V	shear force at cantilever end.
h_0	effective height of section, for beam and column equal to the distance between section compression edge and the point of resultant force of tension reinforcement, for shear wall equal to 0.8 times the section height.
M_n	flexural capacity of RC component.
V_n	shear capacity of RC component according to Chinese code GB 50010-2010.
$V/f_{ck}bh_0$	nominal shear compression ratio.
f_{ck}	characteristic value of concrete compressive strength.
b	width of section.
λ_v	stirrup characteristic value of the component, which can be calculated by $\lambda_v=\rho_{volumn}f_y/f_c$.
ρ_{volumn}	volume stirrup ratio, for beams and columns, it is calculated according to the stirrup in the component, for shear walls, it is calculated according to the stirrup in boundary elements.
f_y	yield strength of stirrup
f_c	axial compressive strength of concrete.
ρ_t	stirrup ratio along the loading direction.
α	confinement effectiveness factor in Mander concrete model.
n	axial load ratio.

Appendix

Table A-1 Failure mode classification criteria of RC beams

Failure mode	Shear span ratio	Flexural shear ratio
Flexural	λ>=2.0	m<=1.0
Shear	λ>=2.0	m>1.0
	λ<2.0	-

Table A-2 Deformation limit of RC beams

Design Parameter			Performance level					
			Intact	Minor Damage	Slight Damage	Moderate Damage	Relatively Severe Damage	Severe Damage
			θ_1	θ_2	θ_3	θ_4	θ_5	θ_6
Flexural								
m	λ_v	$V/f_{ck}bh_0$						
≤0.2	≥0.2	≤0.02	0.004	0.015	0.027	0.038	0.049	0.054
≤0.2	≥0.2	≥0.1	0.004	0.009	0.014	0.019	0.024	0.029
≥0.8	≥0.2	≤0.02	0.005	0.019	0.033	0.046	0.060	0.065
≥0.8	≥0.2	≥0.1	0.005	0.014	0.023	0.031	0.040	0.045
≤0.2	≤0.02	≤0.02	0.003	0.006	0.010	0.013	0.017	0.018
≤0.2	≤0.02	≥0.1	0.003	0.004	0.004	0.005	0.005	0.005
≥0.8	≤0.02	≤0.02	0.005	0.012	0.019	0.025	0.032	0.037
≥0.8	≤0.02	≥0.1	0.005	0.007	0.009	0.011	0.013	0.015
Shear								
m	ρ_t							
≤0.5	≥0.008		0.004	0.009	0.014	0.019	0.024	0.026
≥2.5	≥0.008		0.004	0.007	0.009	0.012	0.014	0.016
≤0.5	≤0.0005		0.004	0.007	0.009	0.012	0.014	0.016
≥2.5	≤0.0005		0.004	0.005	0.007	0.008	0.009	0.012

Table A-3 Failure mode classification criteria of RC columns

Failure mode	Shear span ratio	Flexural shear ratio
Flexural	λ>=2.0	m<=0.6
Flexural-shear	λ>=2.0	0.6<m<=1.0
Shear	λ>=2.0	m>1.0
	λ<2.0	-

Table A-4 Deformation limit of RC columns

Design Parameter			Performance level					
			Intact	Minor Damage	Slight Damage	Moderate Damage	Relatively Severe Damage	Severe Damage
			θ_1	θ_2	θ_3	θ_4	θ_5	θ_6
Flexural								
n	$\alpha\lambda_v$	$V/f_{ck}bh_0$						
≤0.1	≥0.4	≤0.02	0.006	0.014	0.021	0.029	0.036	0.050
≤0.1	≥0.4	≥0.1	0.008	0.022	0.036	0.049	0.063	0.068
≥0.6	≥0.4	≤0.02	0.005	0.011	0.017	0.022	0.028	0.030
≥0.6	≥0.4	≥0.1	0.005	0.011	0.017	0.023	0.029	0.033
≤0.1	≤0.02	≤0.02	0.004	0.010	0.016	0.022	0.028	0.032
≤0.1	≤0.02	≥0.1	0.008	0.018	0.028	0.038	0.048	0.056
≥0.6	≤0.02	≤0.02	0.005	0.005	0.005	0.005	0.005	0.005
≥0.6	≤0.02	≥0.1	0.005	0.010	0.014	0.019	0.023	0.027

Table A-4 Continued

Flexural-shear								
n	ρ_t	m						
≤0.1	≥0.01	≤0.6	0.008	0.017	0.026	0.035	0.044	0.051
≤0.1	≥0.01	≥1.0	0.008	0.016	0.024	0.032	0.04	0.042
≥0.6	≥0.01	≤0.6	0.003	0.007	0.012	0.016	0.02	0.023
≥0.6	≥0.01	≥1.0	0.003	0.008	0.013	0.018	0.023	0.026
≤0.1	≤0.0005	≤0.6	0.006	0.012	0.019	0.025	0.031	0.037
≤0.1	≤0.0005	≥1.0	0.006	0.009	0.013	0.016	0.019	0.022
≥0.6	≤0.0005	≤0.6	0.002	0.003	0.003	0.004	0.004	0.004
≥0.6	≤0.0005	≥1.0	0.002	0.002	0.002	0.002	0.002	0.002
Shear								
n	ρ_t							
≤0.1	≥0.008		0.004	0.007	0.009	0.012	0.014	0.019
≥0.6	≥0.008		0.004	0.006	0.008	0.01	0.012	0.014
≤0.1	≤0.0005		0.003	0.004	0.005	0.006	0.007	0.007
≥0.6	≤0.0005		0.003	0.003	0.003	0.003	0.003	0.003

Table A-5 Failure mode classification criteria of RC shear walls

Failure mode	Shear span ratio	Flexural shear ratio
Flexural	λ>=1.5	m<=1.0
Shear	λ<1.5	-
	λ>=1.5	m>1.0

Table A-6 Deformation limit of RC shear walls

Design Parameter			Performance level					
			Intact	Minor Damage	Slight Damage	Moderate Damage	Relatively Severe Damage	Severe Damage
			θ_1	θ_2	θ_3	θ_4	θ_5	θ_6
Flexural								
n	λ_v	$V/f_{ck}bh_0$						
≤0.1	≥0.35	≤0.02	0.0020	0.0080	0.0130	0.0190	0.0230	0.0270
≤0.1	≥0.35	≥0.1	0.0050	0.0100	0.0150	0.0250	0.0270	0.0290
≥0.4	≥0.35	≤0.02	0.0010	0.0050	0.0100	0.0140	0.0170	0.0200
≥0.4	≥0.35	≥0.1	0.0025	0.0065	0.0105	0.0145	0.0195	0.0205
≤0.1	≤0.05	≤0.02	0.0020	0.0050	0.0080	0.0110	0.0140	0.0160
≤0.1	≤0.05	≥0.1	0.0065	0.0085	0.0115	0.0135	0.0135	0.0135
≥0.4	≤0.05	≤0.02	0.0010	0.0030	0.0050	0.0070	0.0090	0.0090
≥0.4	≤0.05	≥0.1	0.0030	0.0030	0.0030	0.0030	0.0070	0.0070
Shear								
n	m	ρ						
≤0.1	≧2.5	≤0.015	0.0025	0.0055	0.0075	0.0105	0.0125	0.0145
≤0.1	≧2.5	≧0.1	0.0055	0.0075	0.0085	0.0105	0.0115	0.0125
=0.3	≧2.5	≤0.015	0.0025	0.0045	0.0065	0.0085	0.0105	0.0125
=0.3	≧2.5	≧0.1	0.0055	0.0055	0.0055	0.0055	0.0055	0.0055
≤0.1	≤0.5	≤0.015	0.0025	0.0065	0.0115	0.0155	0.0195	0.0205
≤0.1	≤0.5	≧0.1	0.0055	0.0085	0.0105	0.0135	0.0155	0.0155
=0.3	≤0.5	≤0.015	0.0025	0.0055	0.0085	0.0115	0.0145	0.0155
=0.3	≤0.5	≧0.1	0.0055	0.0065	0.0085	0.0095	0.0105	0.0105